

- Ray, W. J., and Koshland, D. E., Jr. (1961), *J. Biol. Chem.* 236, 1973.
- Redkar, V. D., and Kenkare, U. W. (1972), *J. Biol. Chem.* 247, 7576.
- Sharma, C., Manjeshwar, R., and Weinhouse, S. (1963), *J. Biol. Chem.* 238, 3840.
- Shill, J. P., and Neet, K. E. (1971), *Biochem. J.* 123, 283.
- Shill, J. P., Peters, B. A., and Neet, K. E. (1974), *Biochemistry* 13, 3864.
- Subbarao, B., Chakrabarti, U., Redkar, V. D., and Kenkare, U. W. (1973), in *Proceedings of the Symposium on Control Mechanisms in Cellular Processes*, Bhabha Atomic Research Centre, Bombay, February 1-3, p 113.
- Wilson, J. E. (1973), *Arch. Biochem. Biophys.* 159, 543.

## Kinetics of Sulfate Transport by *Penicillium notatum*. Interactions of Sulfate, Protons, and Calcium<sup>†</sup>

John Cuppoletti and Irwin H. Segel\*

**ABSTRACT:** The active transport of inorganic sulfate by an ATP sulfurylase-negative strain of *Penicillium notatum* is promoted by H<sup>+</sup> ions and metal ions (divalent metal ions being more effective than monovalent metal ions). Initial velocity studies suggest that H<sup>+</sup> and SO<sub>4</sub><sup>2-</sup> add to the carrier in an ordered sequence (H<sup>+</sup> before SO<sub>4</sub><sup>2-</sup>), with H<sup>+</sup> at equilibrium with free carrier and carrier-H<sup>+</sup> complex. The linear reciprocal plots and replots suggest a 1:1 stoichiometry between H<sup>+</sup> and SO<sub>4</sub><sup>2-</sup>. Ca<sup>2+</sup> and other divalent metal ions stimulate sulfate transport markedly in buffered suspensions of low ionic strength. The kinetics of the Ca<sup>2+</sup>/SO<sub>4</sub><sup>2-</sup> interaction suggest that Ca<sup>2+</sup> (like H<sup>+</sup>) adds to the carrier before SO<sub>4</sub><sup>2-</sup> and is at equilibrium with free carrier and carrier-Ca<sup>2+</sup> complex. The linear reciprocal plots and replots indicate a 1:1 stoichiometry between Ca<sup>2+</sup> and

SO<sub>4</sub><sup>2-</sup>. Thus the fully loaded carrier-SO<sub>4</sub><sup>2-</sup>-Ca<sup>2+</sup>-H<sup>+</sup> complex has a net positive charge relative to that of the free carrier, a fact consistent with the chemiosmotic hypothesis of membrane transport. The kinetics of the H<sup>+</sup>/Ca<sup>2+</sup> interaction point to a random A-B (rapid equilibrium), ordered C sequence with A = H<sup>+</sup>, B = Ca<sup>2+</sup>, and C = SO<sub>4</sub><sup>2-</sup>. Selenate (an alternate substrate competitive with sulfate) is an uncompetitive inhibitor with respect to Ca<sup>2+</sup>, in agreement with the suggested mechanism. Internal charge balance is not accomplished by a stoichiometric coaccumulation of Ca<sup>2+</sup> and SO<sub>4</sub><sup>2-</sup>. Sulfate transport does, however, promote <sup>45</sup>Ca<sup>2+</sup> uptake. A significant fraction of the added Ca<sup>2+</sup> is bound by the mycelial surface. Binding is extremely rapid, but reversible.

*Penicillium notatum* and related species possess a number of distinct, well-characterized membrane transport systems (Benko et al., 1967, 1969; Bellenger et al., 1968; Tweedie and Segel, 1970; Skye and Segel, 1970; Hackette et al., 1970; Bradfield et al., 1970; Hunter and Segel, 1971; Goldsmith et al., 1973). All of these systems display an obvious pH optimum. In some systems (e.g., amino acid transport), the effect of pH can be related in part to the concentration of the proper ionic form of the substrate (Hunter and Segel, 1971). In other systems (e.g., inorganic sulfate, nitrate, and choline-*O*-sulfate transport), the substrate exists in the same ionic form throughout the pH range tested. In these cases, H<sup>+</sup> must be affecting some component of the transport system. The simplest explanation is that the carrier must exist in the proper ionic form in order to bind and/or translocate the substrate. Thus, a study of the effect of pH on the kinetics of substrate transport may shed some light on the nature of the chemical group(s) at the carrier active site.

The effect of pH on transport rates can be interpreted in another way: there is a good deal of evidence that active membrane transport in microorganisms is energized by a

proton and/or charge gradient across the cell membrane (interior higher pH and/or negative) (Harold, 1972; Hunter and Segel, 1973; Seastron et al., 1973; Slayman and Slayman, 1974). According to this view, a membrane carrier is, in fact, a proton carrier that possesses an additional binding site for a particular solute. H<sup>+</sup> moves inward in response to the membrane potential and the solute is carried along against a concentration gradient. Whether we accept this chemiosmotic explanation for active transport or not, it is possible to apply the principles of enzyme kinetics and consider H<sup>+</sup> and the specific solute as cosubstrates of a bi-reactant system. We can then ask two questions. What is the order of addition of H<sup>+</sup> and the solute to the carrier? What is the stoichiometry between H<sup>+</sup> and the solute (i.e., how many molecules of each combine with the carrier)? The answers to the above questions were the major objectives of this study.

The sulfate transport system of *Penicillium* and *Aspergillus* species differs from others that we have studied in that transport requires a relatively high ionic strength of the incubation medium (Bradfield et al., 1970). In contrast, the fungi will transport neutral and positively charged substrates (e.g., amino acids, choline-*O*-sulfate, and methylammonium) from deionized water (Hackette et al., 1970). The high ionic strength might simply be required to induce the proper conformational state of the sulfate carrier. If this is true, any combination of nontoxic ions should promote

\* From the Department of Biochemistry and Biophysics, University of California, Davis, California 95616. Received May 20, 1975. This work was supported by Grant BMS74-13675 from the National Science Foundation.

transport. On the other hand, positive ions may be required to balance the negative charge of the sulfate ion. In this case, a cation might act as a cosubstrate of the sulfate transport system and some specificity or preference may be observed. If a cation is a cosubstrate, then again we can ask: what is the order of addition of the ligands to the sulfate carrier and what is the stoichiometry between sulfate and cation? An understanding of the role of ionic strength in sulfate transport was another major objective of this study.

### Experimental Section

**Organism and Culture Conditions.** Most experiments were carried out with *Penicillium notatum*, strain 38632R, a white-spored, ATP sulfurylase-negative mutant. This strain is a spontaneous revertant which was isolated from its sulfate transport-negative, ATP sulfurylase-negative parent (listed as strain 38632 by the Commonwealth Mycological Institute and called 38632M in our previous publications). The organism was grown aerobically in submerged culture on a synthetic medium containing L-cysteic acid (0.10 g/l.) as the sole sulfur source (Cuppoletti and Segel, 1974). Growth on low cysteic acid medium derepresses and de-inhibits the sulfate transport system (Bradfield et al., 1970).

**Preparation of Mycelium.** Two-day-old cultures were used for sulfate transport and calcium binding assays. The mycelium (fine, "hairy," microfilamentous, and well-dispersed) was filtered and washed successively with three 300-ml volumes of the following: deionized water, 0.1 M  $K^+$ - $NH_4^+$ -phosphate buffer (pH 6.0), deionized water, 0.01 M  $Na^+$ -EDTA buffer (pH 6.0), and, finally, deionized water. This wash procedure was used to remove any metals bound to the surface of the mycelium. The washed cells were then resuspended to a final concentration of 2.5 g wet weight/100 ml of deionized water and aerated for at least 15 min prior to the assay.

**$^{35}SO_4^{2-}$  Transport Assays.** Transport was measured at room temperature in the following way: a 10-ml aliquot of the suspension of washed mycelium (containing 0.25 g wet weight of cells) was added to 15 ml of appropriate buffer (1.67-fold higher concentration than that desired finally) containing  $^{35}SO_4^{2-}$  (specific activity  $10^7$ - $10^8$  cpm/ $\mu$ mol) and any addition. Rates were calculated from four 2.5-ml aliquots taken at 15-sec intervals after mixing the cells and the labeled substrate. Each sample was filtered rapidly with suction through Whatman No. 1 (1.9 cm) filter paper disks. The resulting mycelial pad was peeled off the filter and counted in a scintillation vial containing 0.5 ml of water (to disperse the mycelium) and 5 ml of scintillation fluid (6 g of 2,5-diphenyloxazole and 100 g of naphthalene/l. of *p*-dioxane). Each aliquot contained 3.5 mg dry weight of mycelium. Since four time samples were used to calculate transport rates, it was unnecessary to wash the mycelium before counting (i.e., there were no complications resulting from different amounts of  $^{35}SO_4^{2-}$  occluded in the mycelial pad at different levels of substrate). Sulfate uptake was linear with time for the duration of the assay.

**Buffers.** The Mes-Tris buffers (indicated as 1 mM, 10 mM, and 50 mM) were prepared by mixing solutions of Mes<sup>1</sup> (2-(*N*-morpholino)ethanesulfonic acid, free acid) with Tris (tris(hydroxymethyl)aminomethane, free base). The concentrations in quotes represent the total concentration of buffer components. For example, the 10 mM buffer was made by mixing 16.7 mM Tris with 16.7 mM Mes to

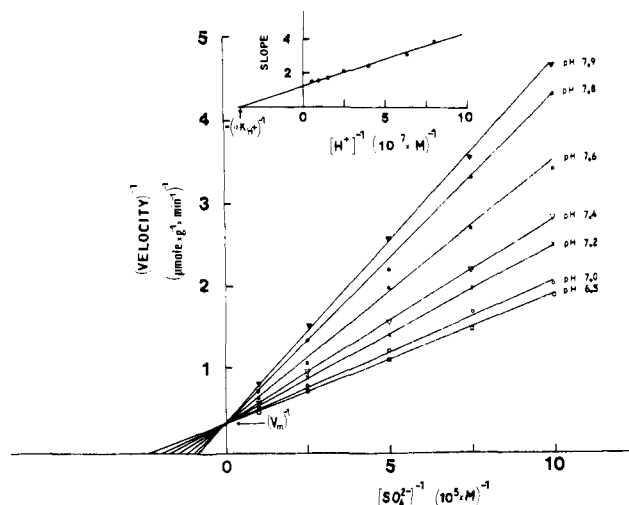


FIGURE 1: Interaction of  $SO_4^{2-}$  and  $H^+$ . Plot of  $1/v$  vs.  $1/[^{35}SO_4^{2-}]$  in the presence of different fixed concentrations of  $H^+$  and 20 mM (saturating)  $CaCl_2$ . The mycelium (suspended in water) was added to a solution containing  $^{35}SO_4^{2-}$  and the appropriate Mes-Tris buffer (10 mM final concentration). The exact hydrogen ion concentration was measured immediately following the 1-min assay using a Radiometer pH meter equipped with a glass electrode. The primary plot yields  $V_{max} = 3.0 \mu\text{mol g}^{-1} \text{min}^{-1}$ . Insert: The slope replot yields  $\alpha K_{H^+} = 2.4 \times 10^{-8} M$ . (The slopes were measured with a ruler and are reported in arbitrary units.) The notation for intercepts and intersection coordinates on this and other figures is based on eq 1.

the desired pH. The actual concentration of Mes and Tris varied according to the pH but the total concentration,  $[Mes] + [Tris]$ , remained 16.7 mM. The buffer was diluted to 10 mM in the assay (see above). The  $K^+$ -barbiturate buffer (pH 4.5) was prepared in the conventional way (by titrating barbituric acid with KOH to the desired pH). The final concentration of free acid plus conjugate base (salt) in the assay mixture was 1 mM. The pH of each assay mixture (including mycelium and any additions) was measured immediately after withdrawal of the last sample.

**$^{45}Ca^{2+}$ -Binding Assays.** The mycelium was harvested and washed as described above and then resuspended at a density of 1 g (wet weight)/100 ml of appropriate buffer.  $^{45}Ca^{2+}$  of known specific activity (ca.  $10^6$  cpm/ $\mu$ mol) was added to the desired final total concentration. Immediately after mixing, a 2.5-ml sample of the suspension was filtered with suction through Whatman No. 1 paper disks (25 mm) or Millipore HA 0.45- $\mu$  nitrocellulose filters (25 mm). The  $[^{45}Ca^{2+}]_{bound}$  was determined by counting the mycelial pad (the pad was not washed). The  $[^{45}Ca^{2+}]_{free}$  was determined by counting an aliquot of the filtrate. The filter paper (which adsorbs a small amount of  $^{45}Ca^{2+}$ ) was also counted and the counts were added to those present in 2.5 ml of filtrate.

**Chemicals.** Carrier-free  $^{35}SO_4^{2-}$  was obtained from Schwartz/Mann and mixed with solutions of unlabeled  $Na_2SO_4$  (or, in one experiment, with  $CaSO_4$ ) to obtain the desired final concentration and specific activity.  $^{45}Ca^{2+}$  (10 Ci/g) and  $^{24}Na^+$  (2.19 Ci/g) were obtained from New England Nuclear and mixed with their respective chloride salts to the desired specific activity. In one experiment, the  $^{45}Ca^{2+}$  was prepared as  $^{45}CaSO_4$ .

### Results

**Interaction of  $H^+$  and  $SO_4^{2-}$ .** A detailed analysis of the effect of pH on sulfate transport is shown in Figure 1. Changing  $[H^+]$  clearly affects the  $K_m$  for sulfate transport,

<sup>1</sup> Abbreviation used is: Mes, 2-(*N*-morpholino)ethanesulfonic acid.

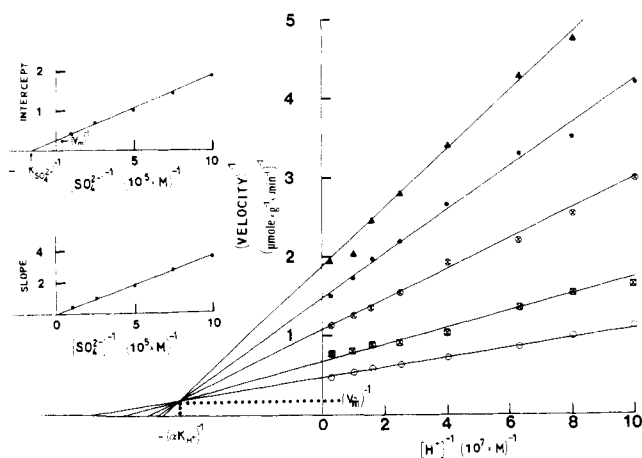


FIGURE 2: Interaction of  $\text{SO}_4^{2-}$  and  $\text{H}^+$ . Plot of  $1/v$  vs.  $1/[\text{H}^+]$  in the presence of different fixed concentrations of  $^{35}\text{SO}_4^{2-}$  and 20 mM (saturating)  $\text{CaCl}_2$ . The fixed  $^{35}\text{SO}_4^{2-}$  concentrations used were:  $1 \times 10^{-6} M$ ,  $1.33 \times 10^{-6} M$ ,  $2 \times 10^{-6} M$ ,  $4 \times 10^{-6} M$ , and  $1 \times 10^{-5} M$ . The experimental conditions were the same as those described in the legend to Figure 1. The primary plot yields  $\alpha K_{H^+} = 2.3 \times 10^{-8} M$ . Inserts: The slope and intercept replots. The intercept replot yields  $V_{\max} = 3.0 \mu\text{mol g}^{-1} \text{min}^{-1}$  and  $K_{\text{SO}_4^{2-}} = 6.3 \times 10^{-6} M$ .

but has no effect on the  $V_{\max}$ . When  $[\text{H}^+]$  is treated as the varied substrate, the family of reciprocal plots intersect to the left of the  $1/v$  axis; both the  $V_{\max}$  and apparent  $K_m$  for  $\text{H}^+$  are affected by changing  $[\text{SO}_4^{2-}]$  (Figure 2). The slope replot is linear but extrapolates to the origin. The pattern is characteristic of a rapid equilibrium ordered sequence (Cleland, 1970; Segel, 1975) with  $\text{H}^+$  adding to the carrier before  $\text{SO}_4^{2-}$ . The linear  $1/v$  vs.  $1/[\text{H}^+]$  plots and the linear slope replot of Figure 1 suggest a 1:1 stoichiometry between  $\text{H}^+$  and  $\text{SO}_4^{2-}$ . Essentially identical results were obtained in preliminary studies where the mycelium was suspended in 0.05 M KCl and where 0.05 M potassium phosphate buffers were used to establish the pH (Cuppoletti and Segel, 1975). Lowendorf et al. (1974) reported a similar effect of changing pH on the  $K_m$  of phosphate transport by *Neurospora crassa*.

**Interaction of  $\text{Ca}^{2+}$  and  $\text{SO}_4^{2-}$ .** Table I shows the effect of various salts on sulfate transport from 1 mM Mes-Tris buffer (pH 6.0). Divalent cations are clearly more effective than monovalent cations. Calcium was chosen for further study because of the availability of  $^{45}\text{Ca}^{2+}$ . Figure 3 shows the concentration dependence of  $\text{Ca}^{2+}$ -promoted and  $\text{Na}^+$ -promoted sulfate transport from 1 mM potassium barbiturate buffer (pH 4.5) ( $\text{pK}_a = 3.98$ ). The differential stimulation cannot be ascribed to a difference in ionic strength. For example, at  $3.33 \times 10^{-5} M$  added  $\text{CaCl}_2$ , the total ionic strength of the incubation solution is  $7.7 \times 10^{-4}$  (three times the molarity of the  $\text{CaCl}_2$  plus  $6.7 \times 10^{-4}$  contributed by the  $\text{K}^+$  and barbiturate $^-$  ions at pH 4.5). The total ionic strength at  $10^{-4} M$  added NaCl is also  $7.7 \times 10^{-4}$ . Yet sulfate transport from the  $\text{CaCl}_2$  solution is 6.5 times faster than transport from the NaCl solution. A more informative comparison is the increase in ionic strength (over that provided by the buffer ions) required to achieve half-maximal sulfate transport. An additional ionic strength of  $3.5 \times 10^{-3}$  is required to obtain 0.5  $V_{\max, \text{app}}$  in the solution containing only monovalent ions; 0.5  $V_{\max, \text{app}}$  is observed at an additional ionic strength of only  $1.2 \times 10^{-4}$  in the  $\text{CaCl}_2$  solution. The differential activity of  $\text{Ca}^{2+}$  and  $\text{Na}^+$  is even more striking than it appears on Figure 3. A substantial fraction of the added  $\text{Ca}^{2+}$  is bound to the mycelium (see below), so

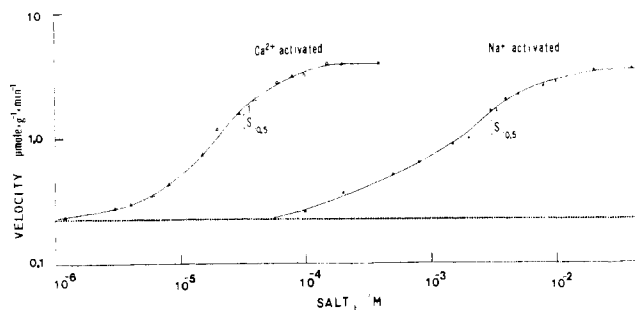


FIGURE 3: Plot of log velocity of sulfate transport vs. log [salt]. The transport assays were run in 1 mM,  $\text{K}^+$ -barbiturate buffer (pH 4.5) containing  $10^{-5} M$   $^{35}\text{SO}_4^{2-}$  (specific activity =  $1.8 \times 10^7$  cpm/ $\mu\text{mol}$ ) and the indicated concentrations of  $\text{CaCl}_2$  or NaCl. The half-maximal velocity for calcium-activated sulfate transport occurs at about  $3.5 \times 10^{-5} M$  (total added)  $\text{Ca}^{2+}$ . The half-maximal velocity for sodium-activated sulfate transport occurs at  $3.5 \times 10^{-3} M$   $\text{Na}^+$  (total added). The dotted line represents the basal rate in the absence of added salt.

Table I: Effect of Different Salts on Sulfate Transport.<sup>a</sup>

Additions ( $10^{-4} M$ )	Sulfate Trans- port Rate, ( $\mu\text{mol g}^{-1}$ $\text{min}^{-1}$ )	Additions ( $10^{-4} M$ )	Sulfate Trans- port Rate, ( $\mu\text{mol g}^{-1}$ $\text{min}^{-1}$ )
None	0.03	$\text{HgCl}_2 + \text{CaCl}_2$	0.98
$\text{MgCl}_2$	1.26	$\text{SnCl}_2$	0.05
$\text{CaCl}_2$	1.45	$\text{SnCl}_2 + \text{CaCl}_2$	1.90
$\text{Ca}(\text{NO}_3)_2$	1.56	$\text{Pb}(\text{NO}_3)_2$	1.04
$\text{Ca}(\text{CH}_3\text{COO})_2$	1.38	$\text{CrCl}_3^c$	2.31
$\text{SrCl}_2$	1.44	$\text{Fe}(\text{NO}_3)_3^c$	0.04
$\text{BaCl}_2$	1.27 <sup>b</sup>	$\text{Fe}(\text{NO}_3)_3 + \text{CaCl}_2^c$	2.02
$\text{MnCl}_2$	1.38	$\text{AlCl}_3^c$	0.09
$\text{FeCl}_2$	1.67	$\text{AlCl}_3 + \text{CaCl}_2^c$	1.36
$\text{CoCl}_2$	1.85	NaCl	0.04
$\text{NiCl}_2$	1.18	KCl	0.04
$\text{CuCl}_2$	0.95	$\text{NH}_4\text{Cl}$	0.04
$\text{ZnCl}_2$	1.03	LiCl	0.04
$\text{CdCl}_2$	1.84	CsCl	0.04
$\text{HgCl}_2$	0.03	Choline-Cl	0.04

<sup>a</sup> Transport was measured in 1 mM Mes-Tris buffer (pH 6.0) containing  $10^{-5} M$   $^{35}\text{SO}_4^{2-}$  and the indicated salts. <sup>b</sup> Theoretically, the  $K_{\text{sp}}$  of  $\text{BaSO}_4$  (ca.  $10^{-10}$ ) should have been exceeded. <sup>c</sup> The pH remained constant at  $6.0 \pm 0.1$  except for  $\text{AlCl}_3$  (pH 5.5),  $\text{Fe}(\text{NO}_3)_3$  (pH 5.5), and  $\text{CrCl}_3$  (pH 5.76).

that the concentration of free  $\text{Ca}^{2+}$  is actually less than that plotted.

A Hill plot for  $\text{Ca}^{2+}$ -activated sulfate transport at pH 4.5 was constructed. If added  $[\text{Ca}^{2+}]$  (i.e.,  $[\text{Ca}^{2+}]_{\text{total}}$ ) is taken as the plotted variable, the slope of the plot in the region of half-apparent  $V_{\max}$  is about 1.46. The  $[\text{Ca}^{2+}]_{0.5, \text{total}}$  is about  $3.8 \times 10^{-5} M$  at  $10^{-5} M$   $^{35}\text{SO}_4^{2-}$ . An independent experiment with  $^{45}\text{Ca}^{2+}$  (described later) established that at low concentrations a significant fraction of the added  $\text{Ca}^{2+}$  was bound to the mycelium. When the  $\text{Ca}^{2+}$  depletion was taken into account (and free  $[\text{Ca}^{2+}]$  taken as the plotted variable), the slope of the Hill plot was about 1.1 with a  $[\text{Ca}^{2+}]_{0.5, \text{free}}$  of about  $2.4 \times 10^{-5} M$ .<sup>2</sup>

Figure 4 shows the effect of different fixed concentrations of  $\text{Ca}^{2+}$  on the kinetics of sulfate transport at pH 4.5

<sup>2</sup> The basis of the Hill plot is the logarithmic form of the Hill equation:  $\log v/(V_{\max} - v) = n \log [S] - \log K'$ , where  $[S]$  represents the concentration of free substrate, which is not necessarily always equal to the concentration of added substrate.

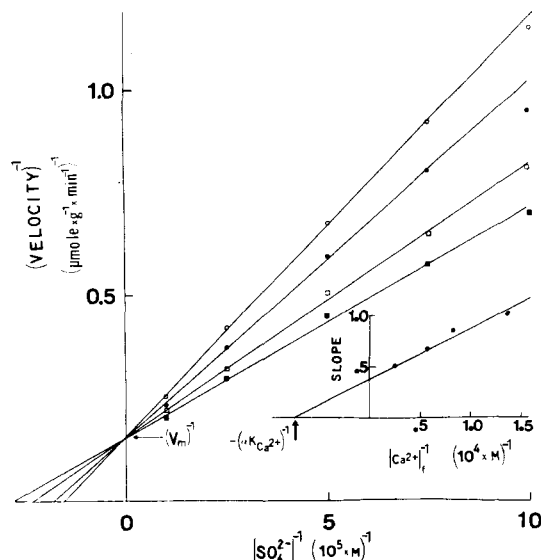


FIGURE 4: Interaction of  $\text{SO}_4^{2-}$  and  $\text{Ca}^{2+}$ . Plot of  $1/v$  vs.  $1/[\text{SO}_4^{2-}]$  at different fixed levels of free  $\text{Ca}^{2+}$  and fixed (saturating)  $[\text{H}^+] = 3.16 \times 10^{-5} \text{ M}$  (pH 4.5). The transport assays were run in 1 mM  $\text{K}^+$ -barbiturate buffer (pH 4.5). The  $[\text{Ca}^{2+}]_{\text{free}}$  was determined as described in Experimental Section. In the concentration range of  $^{35}\text{SO}_4^{2-}$  used ( $10^{-6}$  to  $10^{-5} \text{ M}$   $\text{Na}_2^{35}\text{SO}_4$ ) the  $\text{Na}^+$  had essentially no effect on the  $[\text{Ca}^{2+}]_{\text{free}}/[\text{Ca}^{2+}]_{\text{total}}$  ratio. The primary plot yields  $V_{\text{max}} = 6.7 \mu\text{mol g}^{-1} \text{min}^{-1}$ . The fixed  $[\text{Ca}^{2+}]_{\text{free}}$  concentrations were:  $7.3 \times 10^{-5} \text{ M}$ ,  $1.2 \times 10^{-4} \text{ M}$ ,  $1.7 \times 10^{-4} \text{ M}$ , and  $4 \times 10^{-4} \text{ M}$ . Insert: The slope replot yields  $\alpha K_{\text{Ca}^{2+}} = 1.3 \times 10^{-4} \text{ M}$ .

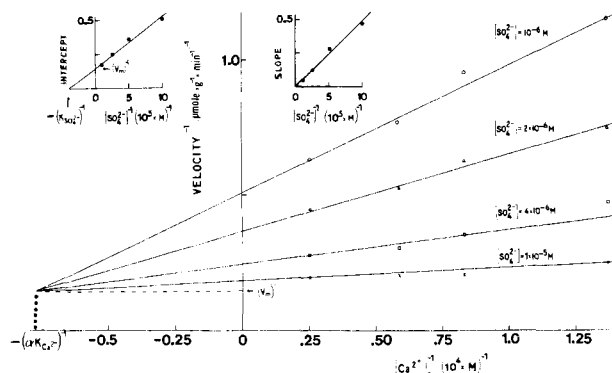


FIGURE 5: Interaction of  $\text{SO}_4^{2-}$  and  $\text{Ca}^{2+}$ . Plot of  $1/v$  vs.  $1/[\text{Ca}^{2+}]$  at different fixed concentrations of  $^{35}\text{SO}_4^{2-}$  and fixed (saturating)  $[\text{H}^+] = 3.16 \times 10^{-5} \text{ M}$  (pH 4.5). The experimental conditions were as described in the legend to Figure 4. The primary plot yields  $\alpha K_{\text{Ca}^{2+}} = 1.3 \times 10^{-4} \text{ M}$ . Inserts: The slope and intercept replots. The intercept replot gives  $K_{\text{SO}_4^{2-}} = 2.5 \times 10^{-6} \text{ M}$ ;  $V_{\text{max}} = 6.7 \mu\text{mol g}^{-1} \text{min}^{-1}$ .

(i.e., saturating  $[\text{H}^+]$ ). The reciprocal plot pattern is similar to that shown for changing fixed  $[\text{H}^+]$ .<sup>3</sup> Figure 5 shows the same data with  $[\text{Ca}^{2+}]_{\text{free}}$  treated as the varied substrate. The slope replot is linear and extrapolates to the origin. The results are consistent with a rapid equilibrium ordered sequence with  $\text{Ca}^{2+}$  adding to the carrier before  $\text{SO}_4^{2-}$ .

**Interaction of  $\text{H}^+$  and  $\text{Ca}^{2+}$ .** The results described above suggest that both  $\text{H}^+$  and  $\text{Ca}^{2+}$  add to the carrier before  $\text{SO}_4^{2-}$ . The experiment described in Figure 1 was conducted

<sup>3</sup> Because there is a basal level of buffer-promoted sulfate transport (in the absence of any added  $\text{Ca}^{2+}$ ), we are actually dealing with a nonessential activation system (Segel, 1975). The slope replot is theoretically hyperbolic. However, in the range of  $[\text{Ca}^{2+}]$  and  $v/V_{\text{max}}$  studied, the system is, for all practical purposes, an obligately bireactant system. That is, the limiting reciprocal plot (at zero  $\text{Ca}^{2+}$ ) is very close to the vertical axis and the slope replot is essentially linear.

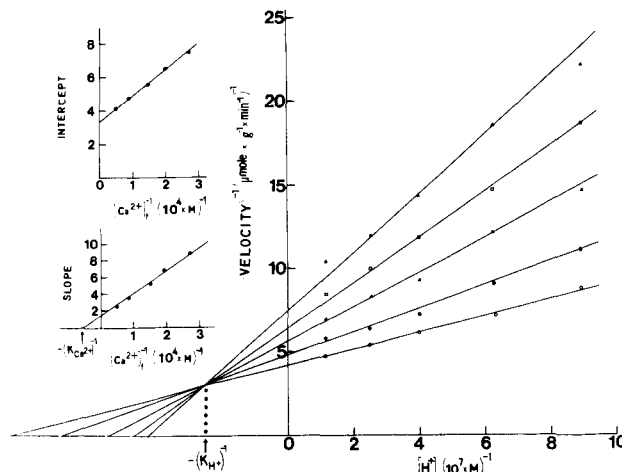


FIGURE 6: Interaction of  $\text{H}^+$  and  $\text{Ca}^{2+}$ . Plot of  $1/v$  vs.  $1/[\text{H}^+]$  at different fixed concentrations of free  $\text{Ca}^{2+}$  and fixed  $[\text{SO}_4^{2-}] = 1 \times 10^{-6} \text{ M}$  (specific activity =  $1.73 \times 10^8 \text{ cpm}/\mu\text{mol}$ ). 10 mM Mes-Tris buffers were used to establish the pH. The primary plot yields  $K_{\text{H}^+} = 4.0 \times 10^{-8} \text{ M}$  ( $\text{p}K_{\text{H}^+} = 7.40$ ). The  $[\text{Ca}^{2+}]_{\text{free}}$  used were:  $3.65 \times 10^{-5} \text{ M}$ ,  $5.2 \times 10^{-5} \text{ M}$ ,  $6.8 \times 10^{-5} \text{ M}$ ,  $1.15 \times 10^{-4} \text{ M}$ , and  $2.0 \times 10^{-4} \text{ M}$  (determined from independent binding assays at pH 7.5 in 10 mM Mes-Tris, as described in Experimental Section). Inserts: The slope and intercept replots. The slope replot yields  $K_{\text{Ca}^{2+}} = 2.0 \times 10^{-4} \text{ M}$ . The intercept replot, if extrapolated to the horizontal axis, gives  $-[1 + ([\text{SO}_4^{2-}]/K_{\text{SO}_4^{2-}})]/\alpha K_{\text{Ca}^{2+}}$ , from which  $\alpha K_{\text{Ca}^{2+}} = 5.5 \times 10^{-5} \text{ M}$  can be calculated (using an average value for  $K_{\text{SO}_4^{2-}}$  of  $4.4 \times 10^{-6} \text{ M}$ ).

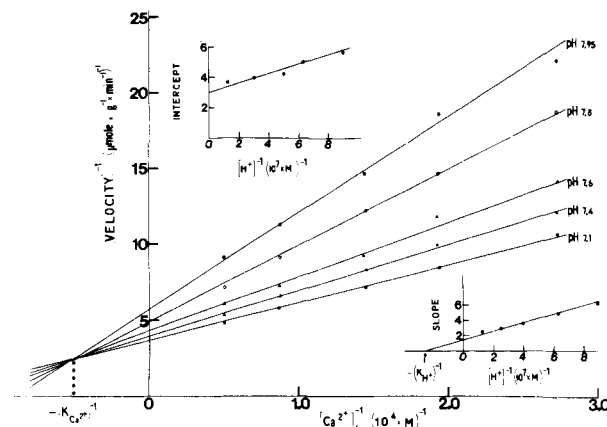


FIGURE 7: Interaction of  $\text{H}^+$  and  $\text{Ca}^{2+}$ . Plot of  $1/v$  vs.  $1/[\text{Ca}^{2+}]$  at different fixed  $[\text{H}^+]$  (10 mM Mes-Tris buffers) and fixed  $[\text{SO}_4^{2-}] = 1 \times 10^{-6} \text{ M}$  (specific activity =  $1.73 \times 10^8 \text{ cpm}/\mu\text{mol}$ ). The primary plot yields  $K_{\text{Ca}^{2+}} = 2.0 \times 10^{-4} \text{ M}$ . Inserts: Slope and intercept replots. The slope replot yields  $K_{\text{H}^+} = 4.0 \times 10^{-8} \text{ M}$ . The intercept replot, if extrapolated to the horizontal axis, gives  $-[1 + ([\text{SO}_4^{2-}]/K_{\text{SO}_4^{2-}})]/\alpha K_{\text{H}^+}$ , from which  $\alpha K_{\text{H}^+} = 1.23 \times 10^{-8} \text{ M}$  can be calculated (using  $K_{\text{SO}_4^{2-}} = 4.4 \times 10^{-6} \text{ M}$ ).

ed in the presence of saturating  $\text{Ca}^{2+}$  (0.02 M). The fact that changing  $[\text{H}^+]$  affects the slope of the  $1/v$  vs.  $1/[\text{SO}_4^{2-}]$  plot at saturating  $[\text{Ca}^{2+}]$  indicates that  $\text{Ca}^{2+}$  does not add between  $\text{H}^+$  and  $\text{SO}_4^{2-}$  in a completely ordered terreactant sequence (Cleland, 1963; Segel, 1975). Similarly, the experiment described by Figure 4 (which was conducted at saturating  $[\text{H}^+]$ ) indicates that  $\text{H}^+$  does not add between  $\text{Ca}^{2+}$  and  $\text{SO}_4^{2-}$  in a completely ordered terreactant sequence. Thus, we can deduce that  $\text{Ca}^{2+}$  and  $\text{H}^+$  add to the carrier in a random fashion. A study of the interaction of  $\text{Ca}^{2+}$  and  $\text{H}^+$  at unsaturating sulfate ( $10^{-6} \text{ M}$ ) is shown in Figures 6 and 7. All replots have finite intercepts. The results are consistent with a rapid equilibrium random addition of  $\text{H}^+$  and  $\text{Ca}^{2+}$  (Segel, 1975). The interaction factor,

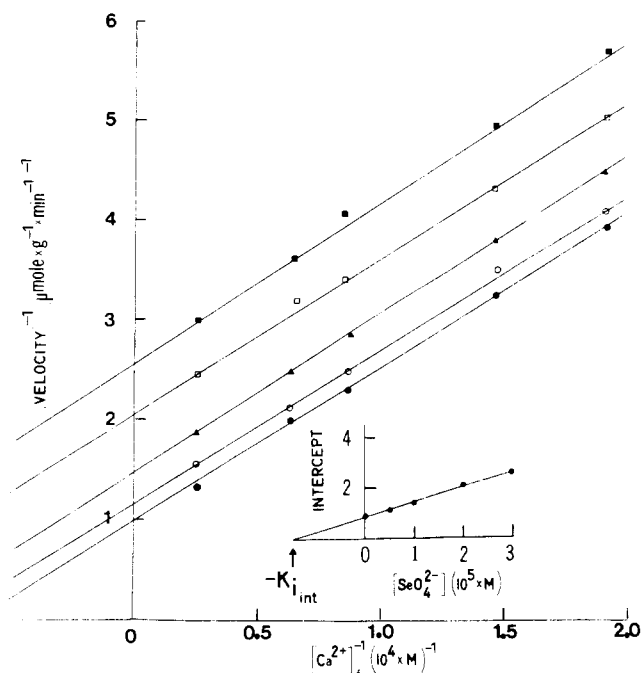


FIGURE 8: Effect of  $\text{SeO}_4^{2-}$  on  $\text{SO}_4^{2-}$  transport. Plot of  $1/v$  vs.  $1/[\text{Ca}^{2+}]_f$  at different fixed concentrations of  $\text{SeO}_4^{2-}$  and a constant  $[\text{SO}_4^{2-}] = 5 \times 10^{-6} M$  (specific activity =  $1 \times 10^7$  cpm/ $\mu\text{mol}$ ). Transport assays (and independent  $^{45}\text{Ca}^{2+}$ -binding assays) were run in 10 mM Mes-Tris buffer (pH 7.5). Insert: The intercept replot yields  $K_{i,\text{int}} = 1.5 \times 10^{-5} M$  where  $K_{i,\text{int}} = K_i[1 + (\alpha K_{H+}/[\text{H}^+]) + ([\text{SO}_4^{2-}]/K_{\text{SO}_4^{2-}})]$  from which  $K_i = 5.9 \times 10^{-6} M$  can be calculated (using  $K_{\text{SO}_4^{2-}} = 4.4 \times 10^{-6} M$  and  $\alpha K_{H+} = 1.23 \times 10^{-8} M$ ).

$\alpha$ , is about 0.29; that is, the binding of one ligand increases the affinity of the carrier for the other by a factor of about 3.4.

**Interaction of  $\text{Na}^+$  and  $\text{SO}_4^{2-}$ .** Experiments using  $^{24}\text{Na}^+$  established that only a negligible fraction of the added  $\text{Na}^+$  bound to the mycelium (in the concentration range where  $\text{Na}^+$  promoted sulfate transport). Nevertheless, the Hill plot for  $\text{Na}^+$ -promoted sulfate transport had a slope of 1.4. Reciprocal plots of  $1/v$  vs.  $1/[\text{Na}^+]$  were nonlinear. The results are consistent with a stoichiometry of 2  $\text{Na}^+$ :1  $\text{SO}_4^{2-}$  (see Discussion).

**Effect of  $\text{SeO}_4^{2-}$ .** Selenate is an alternate substrate of the sulfate transport system (Tweedie and Segel, 1970). In ordered steady-state multireactant systems, an alternate substrate is not very useful as a diagnostic tool. The alternate substrate is competitive with the normal substrate and a linear noncompetitive or mixed-type inhibitor with respect to all cosubstrates, regardless of the order of addition of ligands (Segel, 1975). In rapid equilibrium systems, however, an alternate substrate that adds after the varied substrate acts similarly to a dead end inhibitor (which is useful as a diagnostic tool). Figure 8 shows the effect of  $\text{SeO}_4^{2-}$  on the  $\text{Ca}^{2+}$  dependence of sulfate transport at pH 7.5 (unsaturating  $[\text{H}^+]$ ) and  $5 \times 10^{-6} M$  (unsaturating)  $\text{SO}_4^{2-}$ . Selenate appears to act as an uncompetitive inhibitor with respect to  $\text{Ca}^{2+}$ . The results support the conclusion that  $\text{Ca}^{2+}$  adds to the carrier before  $\text{SO}_4^{2-}$  (or  $\text{SeO}_4^{2-}$ ) and that the  $\text{Ca}^{2+}$  addition step is at equilibrium. Table II summarizes the kinetic constants of the sulfate transport system.

**$^{45}\text{Ca}^{2+}$  Binding to the Mycelium.** As noted earlier, the Hill plot for  $\text{Ca}^{2+}$ -promoted sulfate transport had a slope of  $>1$  when  $\log [\text{Ca}^{2+}]_{\text{total}}$  was taken as the plotted variable. This result prompted us to check for discrepancies between

Table II: Kinetic Constants of the Sulfate Transport System.<sup>a</sup>

Constant	Value <sup>b</sup>
$V_{\text{max}}$	$3.0\text{--}6.7 \mu\text{mol g}^{-1} \text{min}^{-1}$
$K_{H+}$ (i.e., $K_A$ or $K_{ia}$ )	$4.0 \times 10^{-8} M$ ( $\text{p}K_e = 7.40$ )
$\alpha K_{H+}$ (i.e., $\alpha K_A$ or $K_{mA}$ )	$1.23\text{--}2.4 \times 10^{-8} M$ ( $\text{p}K_e' = 7.91\text{--}7.62$ )
$K_{\text{Ca}^{2+}}$ (i.e., $K_B$ or $K_{ib}$ )	$2.0 \times 10^{-4} M$
$\alpha K_{\text{Ca}^{2+}}$ (i.e., $\alpha K_B$ or $K_{mB}$ )	$0.55\text{--}1.3 \times 10^{-4} M$
$\alpha$ (calculated interaction factor: $K_{mA}/K_{ia} = K_{mB}/K_{ib}$ )	ca. 0.29 <sup>c</sup>
$K_{\text{SO}_4^{2-}}$ (i.e., $K_C$ or $K_{mC}$ )	$2.5\text{--}6.3 \times 10^{-6} M$
$K_{\text{SeO}_4^{2-}}$ (i.e., $K_i$ or $K_{mI}$ )	$5.9 \times 10^{-6} M$

<sup>a</sup> The various kinetic constants were obtained from the replots and intersection coordinates of Figures 1, 2, and 4–8. <sup>b</sup> Several constants were obtained from two or three different plots. The range shows the minimum and maximum values obtained. Some of the variation stems from (a) the fact that  $\text{H}^+$  ion concentrations were calculated from pH measurements made with a glass electrode (which cannot be read closer than 0.02 unit); (b) there were slight variations in the degree of derepression of different batches of mycelium (which would affect  $V_{\text{max}}$  values), and (c) the room temperature varied by as much as  $7^\circ$  from day to day. To minimize the effect of (b) and (c), all the data for any complementary pair of reciprocal plots were obtained with the same batch of mycelium on the same day. <sup>c</sup> From Figures 6 and 7.

$[\text{Ca}^{2+}]_{\text{total}}$  and  $[\text{Ca}^{2+}]_{\text{free}}$ . Studies with  $^{45}\text{Ca}^{2+}$  indicated that a substantial fraction of the added calcium is bound to the mycelium.  $^{45}\text{Ca}^{2+}$  binding is extremely rapid—samples taken a few seconds after adding the  $^{45}\text{Ca}^{2+}$  are completely equilibrated. Similarly, when mycelium containing bound  $^{45}\text{Ca}^{2+}$  is filtered and resuspended in fresh buffer, the  $^{45}\text{Ca}^{2+}$  reequilibrates immediately. This suggests that the  $^{45}\text{Ca}^{2+}$  is reversibly adsorbed to the surface of the mycelium, rather than actively transported into the cytoplasm. A reciprocal plot and a Hill plot for  $^{45}\text{Ca}^{2+}$  binding at pH 6.0 were constructed. Half-maximal saturation was observed at a free  $[\text{Ca}^{2+}]$  of about  $1.3 \times 10^{-5} M$ . At saturation, approximately 60  $\mu\text{mol}$  of  $\text{Ca}^{2+}$  was bound per g dry weight of mycelium. The Hill plot was linear with a slope of about 0.9 (when  $\log \text{free } [\text{Ca}^{2+}]$  was the plotted variable).

The effect of unlabeled cations on  $^{45}\text{Ca}^{2+}$  binding was determined. Aerated mycelia in 1 mM Mes-Tris buffer (pH 6.0) were preincubated for 1 min with  $10^{-4} M$   $^{45}\text{CaCl}_2$  (specific activity  $1.07 \times 10^6$  cpm/ $\mu\text{mol}$ ). Potential competing cations (as chlorides) were added to a final concentration of  $10^{-4} M$ . After an additional minute, duplicate 2.5-ml samples (containing 3.5 mg dry weight of mycelium) were rapidly filtered and counted. All the divalent metal ions tested ( $\text{Mg}^{2+}$ ,  $\text{Sr}^{2+}$ ,  $\text{Mn}^{2+}$ ,  $\text{Co}^{2+}$ , and  $\text{Ba}^{2+}$ ) were about as effective as unlabeled  $\text{Ca}^{2+}$  in displacing bound  $^{45}\text{Ca}^{2+}$  (31–41% inhibition of  $^{45}\text{Ca}^{2+}$  binding). Monovalent cations ( $\text{Na}^+$ ,  $\text{K}^+$ ,  $\text{Li}^+$ ,  $\text{Cs}^+$ , and  $\text{NH}_4^+$ ) inhibited  $^{45}\text{Ca}^{2+}$  binding by only 1–14%. Essentially identical results were obtained when the order of addition of  $^{45}\text{Ca}^{2+}$  and competing cation was reversed. The  $K_i$  for  $\text{Mg}^{2+}$  as an inhibitor of  $^{45}\text{Ca}^{2+}$  binding is about  $1.6 \times 10^{-5} M$ , as determined from a linear plot described by Best-Belpomme and Dessen (1973).<sup>4</sup>

<sup>4</sup> The Best-Belpomme and Dessen plot permits total substrate and total inhibitor concentrations to be plotted. The usual plot of  $1/[\text{Ca}^{2+}]_{\text{bound}}$  vs.  $1/[\text{Ca}^{2+}]_{\text{free}}$  (or a Scatchard plot) in the presence and in the absence of a fixed concentration of free  $\text{Mg}^{2+}$  could not be constructed because it was impossible to maintain  $[\text{Mg}^{2+}]_{\text{free}}$  constant as  $[\text{Ca}^{2+}]_{\text{free}}$  was varied.

Table III: Mycelial  $^{35}\text{SO}_4^{2-}$  and  $^{45}\text{Ca}^{2+}$  Content after Incubation with  $\text{Ca}^{35}\text{SO}_4$ ,  $^{45}\text{CaSO}_4$ , or  $^{45}\text{CaCl}_2$ .<sup>a</sup>

Incubation Medium ( $10^{-3} M$ )	Labeled Ion in Mycelium ( $\mu\text{mol/g}$ ) <sup>b</sup>			
	Strain 38632R		Strain 38632M	
	1–2 min	4 hr	1–2 min	4 hr
$\text{Ca}^{35}\text{SO}_4$	7	187	1.5	1.5
$^{45}\text{CaSO}_4$	39	110	35	64
$^{45}\text{CaCl}_2$	44	67	46	65

<sup>a</sup> Washed mycelia of *P. notatum*, strain 38632R (sulfate transport-positive), and of *P. notatum*, strain 38632M (sulfate transport-negative), were suspended at a density of 1 g (wet weight)/100 ml in deionized water containing one of the above labeled salts (specific activity  $1-2 \times 10^5$  cpm/ $\mu\text{mol}$ ). Periodically, 5.0-ml aliquots were removed and filtered, and the mycelium was counted. The mycelial content of  $^{35}\text{SO}_4^{2-}$  and  $^{45}\text{Ca}^{2+}$  after 1–2 min and after 4 hr of incubation are shown. <sup>b</sup> Dry weight basis.

**Is There Coaccumulation of Sulfate and Calcium?** The avid instantaneous binding of  $^{45}\text{Ca}^{2+}$  to the mycelial surface made it impossible to study the kinetics of calcium uptake. (The high zero-time values obscured any small increments of mycelial  $^{45}\text{Ca}^{2+}$  that might have occurred over the relatively short incubation times required for accurate initial velocity studies.) Nevertheless, an attempt was made to determine if  $\text{Ca}^{2+}$  is cotransported with  $\text{SO}_4^{2-}$  (or if  $\text{Ca}^{2+}$  serves only to promote  $\text{SO}_4^{2-}$  binding). Table III shows the levels of  $^{35}\text{SO}_4^{2-}$  and  $^{45}\text{Ca}^{2+}$  in (and on) the mycelium of strain 38632R (sulfate transport positive) and in (and on) the mycelium of strain 38632M (sulfate transport negative) after 1–2 min and after prolonged incubation with  $\text{Ca}^{35}\text{SO}_4$  or  $^{45}\text{CaSO}_4$  or  $^{45}\text{CaCl}_2$ . Strain 38632M rapidly adsorbed approximately 40  $\mu\text{mol}$  of  $^{45}\text{Ca}^{2+}$  per g dry weight of mycelium from either  $^{45}\text{CaSO}_4$  or  $^{45}\text{CaCl}_2$ . The amount rose to about 65  $\mu\text{mol/g}$  after 4 hr. The difference between the 1–2-min values and the 4-hr values represents sulfate-independent  $\text{Ca}^{2+}$  uptake (or exchange). Strain 38632R also adsorbed about 40  $\mu\text{mol}$  of  $^{45}\text{Ca}^{2+}$  per g from either salt within the first 1–2 min. By 4 hr, the mycelial  $^{45}\text{Ca}^{2+}$  obtained from  $^{45}\text{CaCl}_2$  rose to 67  $\mu\text{mol/g}$  (the same as in the sulfate transport-negative strain). However, when the  $^{45}\text{Ca}^{2+}$  was present as  $^{45}\text{CaSO}_4$ , the mycelial  $^{45}\text{Ca}^{2+}$  increased to 110  $\mu\text{mol/g}$ . It is clear that sulfate promotes  $^{45}\text{Ca}^{2+}$  uptake provided the sulfate is transported. However, the  $\text{Ca}^{2+}/\text{SO}_4^{2-}$  accumulation ratio is only 0.23:1 (43  $\mu\text{mol/g}$  “excess” of  $\text{Ca}^{2+}$  per 187  $\mu\text{mol/g}$  of  $\text{SO}_4^{2-}$ ).

## Discussion

The cumulative data suggest that the kinetic mechanism of the sulfate transport system of *P. notatum* is random A–B (rapid equilibrium), ordered C with  $\text{H}^+ = \text{A}$ ,  $\text{Ca}^{2+} = \text{B}$ , and  $\text{SO}_4^{2-} = \text{C}$ . The binding sequence is shown in Figure 9. The velocity equation (assuming that C and EABC are included in the rapid equilibrium segment) is (Segel, 1975):

$$\frac{v}{V_{\max}} = \frac{[\text{A}][\text{B}][\text{C}]/\alpha K_A K_B K_C}{1 + [\text{A}]/K_A + [\text{B}]/K_B + [\text{A}][\text{B}]/\alpha K_A K_B + [\text{A}][\text{B}][\text{C}]/\alpha K_A K_B K_C} \quad (1)$$

If the sulfate addition step is not at equilibrium, the form of the equation is unchanged, but the constant associated with C is  $K_{\text{mc}}$  (a kinetic constant composed of several rate constants), rather than the dissociation constant,  $K_C$ . Considering the nature of the process, it seems likely that translo-

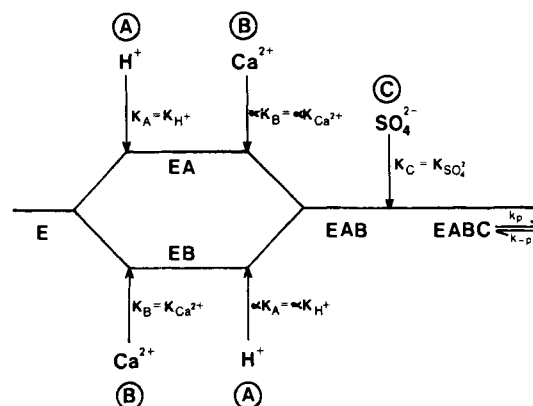


FIGURE 9: Proposed kinetic mechanism for  $\text{Ca}^{2+}$ - and  $\text{H}^+$ -promoted sulfate transport in *Penicillium notatum*. The alternate Cleland notation is shown in Table II.

cation is the slowest and rate-limiting step. In this case, all the complexes shown in Figure 9 would be at equilibrium.

The effect of  $\text{H}^+$  on sulfate transport should not be a source of excessive speculation. The fact that changing pH affects the  $K_m$  for sulfate, but not  $V_{\max}$ , simply means that (a)  $\text{SO}_4^{2-}$  binds only to a protonated carrier and (b) the binding and dissociation of  $\text{H}^+$  are very rapid compared to some subsequent step. The linear reciprocal plots and re-plots establish a 1:1 stoichiometry between  $\text{H}^+$  and  $\text{SO}_4^{2-}$ , but the results do not prove that  $\text{H}^+$  translocation is the driving force for sulfate transport. On the other hand, the results are not inconsistent with the chemiosmotic hypothesis—a higher internal pH would reduce the effective affinity of the carrier for sulfate.

The role of  $\text{Ca}^{2+}$  (or another divalent cation) is unclear. The simplest interpretation is that  $\text{Ca}^{2+}$  promotes  $\text{SO}_4^{2-}$  binding to the carrier by neutralizing negative (repulsive) charges. The fact that the quaternary carrier- $\text{H}^+$ - $\text{Ca}^{2+}$ - $\text{SO}_4^{2-}$  complex has a net positive charge (over that of the free carrier) is also consistent with the chemiosmotic hypothesis: even though the substrate is negatively charged, the fully loaded carrier would move inward in response to an electrochemical potential (interior negative). The conclusion that the quaternary complex must have a net positive charge over that of the free carrier is supported by the data for  $\text{Na}^+$ -promoted sulfate transport. The slope of the Hill plot is about 1.4, suggesting that two  $\text{Na}^+$  ions are bound to the carrier. In fact, an ordered addition of two  $\text{Na}^+$  ions to sites with the same intrinsic  $K_S$  values would yield an apparent  $n$  value of 1.36; a random addition of two  $\text{Na}^+$  to sites with the same intrinsic  $K_S$  values would yield an apparent  $n$  value of 1.2 (Segel, 1975). It is noteworthy that both  $\text{H}^+$  and a metal ion are required. That is, three  $\text{K}^+$  ions will not substitute for two  $\text{K}^+$  ions and an  $\text{H}^+$  ion. (Sulfate transport is still pH-dependent at 0.1 M  $\text{K}^+$ ) (Cuppoletti and Segel, 1975). Also,  $\text{Cr}^{3+}$ -activated sulfate transport is pH-dependent. The cotransport of cations along with anionic substrates may be a general phenomenon in

microorganisms (Halpern et al., 1973; Komor and Tanner, 1974; Cockburn et al., 1975; Harold and Spitz, 1975).

Although the kinetic stoichiometry between  $\text{SO}_4^{2-}$  and  $\text{Ca}^{2+}$  is 1:1, the amount of  $^{45}\text{Ca}^{2+}$  accumulated by the mycelium (over and above that adsorbed to the surface) is only

23% of the  $^{35}\text{SO}_4^{2-}$  accumulated. Thus, it appears that  $\text{Ca}^{2+}$  plays a role in the translocation process, but internal charge balance is not accomplished by a coaccumulation of  $\text{Ca}^{2+}$  along with  $\text{SO}_4^{2-}$ . This suggests that most of the translocated  $\text{Ca}^{2+}$  returns with the unloaded carrier to the external side of the membrane. It is likely then that the sulfate carrier operates as an anion exchanger, translocating sulfate inward and an anion (e.g.,  $\text{OH}^-$ ,  $\text{HPO}_4^{2-}$ ) outward (perhaps as the neutral carrier- $\text{Ca}^{2+}$ - $\text{HPO}_4^{2-}$  complex). The excess mycelial  $^{45}\text{Ca}^{2+}$  taken up from  $^{45}\text{CaSO}_4$  probably results from equilibration of the carrier- $^{45}\text{Ca}^{2+}$  complex with an internal pool of unlabeled  $\text{Ca}^{2+}$ ,  $\text{Mg}^{2+}$ , etc., the total concentration of intracellular cations remaining unchanged.

It is unlikely that all the  $\text{Ca}^{2+}$ -binding substance on the mycelial surface is identical with the sulfate carrier. For one thing, there is simply too much of the material present (ca. 60  $\mu\text{mol}$  of binding sites per g dry weight of mycelium). Furthermore,  $^{45}\text{Ca}^{2+}$  binding was equally avid in mycelium fully repressed for the sulfate transport system (by growth on excess L-methionine) (Bradfield et al., 1970) and in the sulfate transport-negative mutant, strain 38632M. In fact, all strains of *P. notatum*, *P. chrysogenum*, and *Aspergillus nidulans* that were tested bound  $^{45}\text{Ca}^{2+}$  equally well. The washed, insoluble debris of broken cells also bound  $^{45}\text{Ca}^{2+}$  (while  $^{35}\text{SO}_4^{2-}$  transport or binding was nil). The  $\text{Ca}^{2+}$ -binding material may be identical with the low molecular weight glycopeptide that Le'John et al. (1974) reported in *Achlya*, another filamentous fungus. This glycopeptide binds 20 atoms of  $\text{Ca}^{2+}$ /molecule. The fact that the  $\text{Ca}^{2+}$ -binding material is distinct from the sulfate carrier does not rule out a role for this substance in anion transport or retention.

#### References

- Bellenger, N., Nissen, P., Wood, T., and Segel, I. H. (1968), *J. Bacteriol.* 96, 1574.
- Benko, P. V., Wood, T., and Segel, I. H. (1967), *Arch. Biochem. Biophys.* 122, 783.
- Benko, P. V., Wood, T. C., and Segel, I. H. (1969), *Arch. Biochem. Biophys.* 129, 498.
- Best-Belpomme, M., and Dessen, P. (1973), *Biochimie* 55, 11.
- Bradfield, G., Somerfield, P., Meyn, T., Holby, M., Babcock, D., Bradley, D., and Segel, I. H. (1970), *Plant Physiol.* 46, 720.
- Cleland, W. W. (1963), *Biochim. Biophys. Acta* 67, 188.
- Cleland, W. W. (1970), *Enzymes*, 3rd Ed. 2, 1.
- Cockburn, M., Earnshaw, P., and Eddy, A. A. (1975), *Biochem. J.* 146, 705.
- Cuppoletti, J., and Segel, I. H. (1974), *J. Membr. Biol.* 17, 239.
- Cuppoletti, J., and Segel, I. H. (1975), *J. Theor. Biol.* (in press).
- Goldsmith, J., Livoni, J., and Segel, I. H. (1973), *Plant Physiol.* 52, 362.
- Hackette, S. L., Skye, G. E., Burton, C., and Segel, I. H. (1970), *J. Biol. Chem.* 245, 4241.
- Halpern, Y. S., Barash, H., Dover, S., and Druck, K. (1973), *J. Bacteriol.* 114, 53.
- Harold, F. M. (1972), *Bacteriol. Rev.* 36, 172.
- Harold, F. M., and Spitz, E. (1975), *J. Bacteriol.* 122, 266.
- Hunter, D. R., and Segel, I. H. (1971), *Arch. Biochem. Biophys.* 144, 168.
- Hunter, D. R., and Segel, I. H. (1973), *J. Bacteriol.* 113, 1184.
- Komor, E., and Tanner, W. (1974), *Eur. J. Biochem.* 44, 219.
- Le'John, H. B., Cameron, L. E., Stevenson, R. M., and Meusen, R. U. (1974), *J. Biol. Chem.* 249, 4016.
- Lowendorf, H. S., Slayman, C. L., and Slayman, C. W. (1974), *Biochim. Biophys. Acta* 373, 369.
- Seastron, A., Inkson, C., and Eddy, A. A. (1973), *Biochem. J.* 134, 1031.
- Segel, I. H. (1975), *Enzyme Kinetics: Behavior and Analysis of Rapid Equilibrium and Steady-State Enzyme Systems*, New York, N.Y., Wiley-Interscience.
- Skye, G. E., and Segel, I. H. (1970), *Arch. Biochem. Biophys.* 138, 306.
- Slayman, C. L., and Slayman, C. W. (1974), *Proc. Natl. Acad. Sci. U.S.A.* 71, 1935.
- Tweedie, J., and Segel, I. H. (1970), *Biochim. Biophys.*